

Quantum molecular dynamics study of fusion and its fade out in the $^{16}\text{O} + ^{16}\text{O}$ system

Toshiki Maruyama, Akira Ohnishi, and Hisashi Horiuchi

Department of Physics, Kyoto University, Kyoto 606, Japan

(Received 12 December 1989)

The quantum molecular dynamic method is used to study the fusion reaction in the $^{16}\text{O} + ^{16}\text{O}$ system and its fade out with the increase of the incident energy. It is shown that without two-nucleon collisions there appears the so-called fusion window, as in the time-dependent Hartree-Fock approach, while with the inclusion of two-nucleon collisions the low partial wave cutoff in fusion disappears. The fade out of the fusion process with the increase of the incident energy is found to be due to the increase of the cross sections mainly of the incomplete fusion process in the whole range of the impact parameter and partly of the deep-inelastic-collision-like process in the peripheral region. The calculated fusion cross section as a function of incident energy is shown to be in good accordance with experiments.

I. INTRODUCTION

The microscopic model which is dubbed quantum molecular dynamics (QMD) by Aichelin and Stöcker has been devised and developed as one of the numerical simulation methods to study medium- and high-energy heavy-ion reactions.¹⁻⁴ The simulation approach⁵⁻⁸ by Boal and his collaborators can be regarded to be essentially the same as the QMD. The difference between the QMD and the traditional molecular dynamics is that the former incorporates the stochastic two-nucleon collision process.⁹⁻¹¹ The QMD method simulates heavy-ion reactions on an event-by-event basis, and as a consequence, incorporates many-nucleon correlations. Therefore this model offers us an opportunity to calculate not only one-body observables but also fragment formation.

Until now, however, the QMD method has not been used to study the reaction processes in low-energy region including the fusion process and it has been scarcely used even in the Fermi energy region, $E_{\text{lab}} \sim 30$ MeV/nucleon, where E_{lab} stands for the incident energy in the laboratory frame. This, the present authors consider, is mainly due to the insufficient stability of the projectile and target nuclei constructed in the framework of the QMD method. Recently the present authors have succeeded to construct in the QMD framework the stable nuclei which maintain their stability, usually more than 2000 fm/c.¹² Therefore now we are able to use the QMD method to study the low-energy heavy-ion collision processes and also the evolution of the collision mechanism from the low-energy region to the medium-energy one. Since the onset of the fragmentation mechanism is considered to be an important ingredient for the collision mechanism evolution, it is very interesting and important to study how the heavy-ion collision processes are described in the framework of the QMD method in low and Fermi energy regions.

In this paper we report the results of the study of the fusion reaction and its fade out in the $^{16}\text{O} + ^{16}\text{O}$ system in the framework of the QMD. This study shows us through what kinds of mechanism the fusion process

fades out in the light heavy-ion system as the incident energy increases from low to medium. The reliability of our QMD approach is guaranteed by the result that the calculated fusion cross section as a function of the incident energy is in good accordance with experiments. We have also studied the role of two-nucleon collisions. When two-nucleon collisions are switched off we observe the appearance of the so-called fusion window as in the TDHF (time-dependent Hartree-Fock) approach, but with the inclusion of two-nucleon collisions nowhere do we see the fusion window.

This paper is organized as follows. The description of equation of motion together with the presentation of parameter values and the explanation of the initialization are given in Sec. II. Results of the study of the fusion reaction with exclusion of two-nucleon collisions are given in Sec. III. The study of the fusion process and its fade out is made in Sec. IV. We will see that the decrease of the fusion cross section with the increase of the incident energy is due to the increase of the cross section mainly of the incomplete fusion process in the whole range of the impact parameter and partly of the deep-inelastic-collision-like process in the peripheral region. There it is shown that the reproduction of the experimental fusion cross section by the theory is good. Finally in Sec. V, summary and discussions are given. There we report also some preliminary results about the evolution of the collision mechanism after the fade out of the fusion process.

II. MOTION OF WAVE PACKETS AND INITIALIZATION

A. Motion of wave packets

In the QMD method we assign a Gaussian wave packet to each nucleon in the phase space, and the sum of all the wave packets gives us a one-body distribution function $f(\mathbf{r}, \mathbf{p})$ in the phase space,

$$f(\mathbf{r}, \mathbf{p}) = \sum_i \delta \exp[-(\mathbf{r} - \mathbf{r}_i)^2/L^2 - (\mathbf{p} - \mathbf{p}_i)^2L^2/\hbar^2] \quad (2.1)$$

which is normalized as

$$\int \frac{d^3r d^3p}{(2\pi\hbar)^3} f(\mathbf{r}, \mathbf{p}) = \text{mass number} . \quad (2.2)$$

The width parameter L is fixed independent of time and in this paper we have chosen $L = 1.73$ fm. The time evolution of the phase space point $(\mathbf{r}_i, \mathbf{p}_i)$ for each nucleon consists of the propagation governed by the Newtonian equation of motion and of stochastic two-nucleon collisions. The Newtonian equation of motion is derived from the following Hamiltonian H ,

$$H = \sum_i \frac{p_i^2}{2m} + \frac{1}{2} \frac{\alpha}{\rho_0} \sum_i \langle \rho_i \rangle + \frac{1}{2+\sigma} \frac{\beta}{\rho_0^{\sigma+1}} \sum_i \langle \hat{\rho}_i \rangle^{\sigma+1} + \frac{1}{2} \sum_{i \neq j} \frac{(e/2)^2}{|\mathbf{r}_i - \mathbf{r}_j|} \text{erfc}(|\mathbf{r}_i - \mathbf{r}_j|/\sqrt{2} \cdot L) , \quad (2.3)$$

where

$$\begin{aligned} \langle \rho_i \rangle &\equiv \sum_{j \neq i} (2\pi L^2)^{-3/2} \exp[-(\mathbf{r}_j - \mathbf{r}_i)^2/2L^2] \\ &= \sum_{j \neq i} \int d^3r_1 d^3r_2 (\pi L^2)^{-3/2} \exp[-(\mathbf{r}_1 - \mathbf{r}_i)^2/L^2] \\ &\quad \times \delta(\mathbf{r}_1 - \mathbf{r}_2) (\pi L^2)^{-3/2} \\ &\quad \times \exp[-(\mathbf{r}_2 - \mathbf{r}_j)^2/L^2] , \\ \langle \hat{\rho}_i \rangle &\equiv \sum_{j \neq i} (2\pi \hat{L}^2)^{-3/2} \exp[-(\mathbf{r}_j - \mathbf{r}_i)^2/2\hat{L}^2] . \end{aligned} \quad (2.4)$$

The second and third terms in H take the following form in the limit of nuclear matter:

$$\frac{1}{2} \frac{\alpha}{\rho_0} \int d^3r [\rho(\mathbf{r})]^2 + \frac{1}{2+\sigma} \frac{\beta}{\rho_0^{\sigma+1}} \int d^3r [\rho(\mathbf{r})]^{\sigma+2} , \quad (2.5)$$

where $\rho(\mathbf{r})$ stands for the nuclear matter constant density. This is the potential energy due to the widely used simplified Skyrme-type effective nuclear force.¹³⁻¹⁵ In this paper we have adopted $\rho_0 = 0.165$ fm⁻³, $\sigma = 1$, $\alpha = -124$ MeV, and $\beta = 70.5$ MeV which give for the nuclear matter proper binding energy $E = -16$ MeV but stiff incompressibility $K = 378$ MeV. $\langle \hat{\rho}_i \rangle$ is the same as $\langle \rho_i \rangle$ if the width parameter \hat{L} of $\langle \hat{\rho}_i \rangle$ is taken to be the same as L . In this paper we have chosen $\hat{L}^2 = 0.8125L^2$. This choice has been made in order to adjust the effect of the repulsive density-dependent force.

The last term in H is the Coulomb potential energy which is derived by imposing, for the sake of simplicity, $e/2$, half the elementary charge, to every nucleon. In deriving this term we used the following relation:

$$\begin{aligned} &\int d^3r_1 d^3r_2 (\pi L^2)^{-3/2} \exp[-(\mathbf{r}_1 - \mathbf{r}_i)^2/L^2] \\ &\quad \times \frac{(e/2)^2}{|\mathbf{r}_1 - \mathbf{r}_2|} (\pi L^2)^{-3/2} \exp[-(\mathbf{r}_2 - \mathbf{r}_j)^2/L^2] \\ &= \frac{(e/2)^2}{|\mathbf{r}_i - \mathbf{r}_j|} \text{erfc}(|\mathbf{r}_i - \mathbf{r}_j|/\sqrt{2} \cdot L) , \end{aligned} \quad (2.6)$$

$$\text{erfc}(A) \equiv (2/\sqrt{\pi}) \int_0^A dx e^{-x^2} .$$

The stochastic two-nucleon collision is treated as fol-

lows. Two nucleons are scattered if they come closer than the distance $r_{NN} \equiv \sqrt{\sigma_{NN}/\pi}$ where σ_{NN} is the total nucleon-nucleon cross section. The scattering angle is chosen randomly so that the scattering is isotropic. In this paper, σ_{NN} in the nuclear medium has been chosen to be 30 mb independently of the energy. The scattering is Pauli blocked with the probability P_{block} which stands for the probability that the final state of the scattering is occupied by other nucleons. Since the nucleon has four internal degrees of freedom (spin and isospin), P_{block} is expressed as follows

$$P_{\text{block}} = 1 - [1 - \frac{1}{4} f(\mathbf{r}_i, \mathbf{p}'_i)] [1 - \frac{1}{4} f(\mathbf{r}_j, \mathbf{p}'_j)] , \quad (2.7)$$

where \mathbf{p}'_i and \mathbf{p}'_j are the momenta of the two nucleons (i and j) in the final state of the scattering.

Newtonian equation is solved numerically using the first-order difference equation with a fixed time step $\Delta t = 0.2$ fm/c.^{2,3} The total energy is checked to be conserved within the numerical error of 1 MeV during the time span of 500 fm/c.

B. Initialization

One basic requirement that the QMD model has to fulfill is the stability of the projectile and target nuclei. The stability of the nucleus means that the nucleus experiences no nucleon escape and its root-mean-square (rms) radius remains almost constant with small fluctuation. This stability should last at least on a time scale compatible with the time span during which the collision dynamics under consideration evolves in time sufficiently. Recently the present authors have succeeded to construct the stable nuclei which maintain their stability usually more than 2000 fm/c. The construction of stable nucleus is made by the application of the cooling method to the nucleus composed by the Monte Carlo sampling of nucleon coordinates and momenta. The cooling method is to deexcite nucleus to its ground state by means of reducing the relative momentum of two nucleons at each collision process. The reduction of relative momentum is allowed only when it is not Pauli blocked. The details of this cooling method will be reported elsewhere.¹²

The ¹⁶O nucleus which we have constructed by using the Hamiltonian of Eq. (2.3) keeps its stability for more than 3000 fm/c in both cases where two-nucleon collisions are switched on and switched off. The ¹⁶O nucleus we have constructed has its binding energy, -141 MeV and its rms radius, about 2.9 fm. Figure 1 shows the time

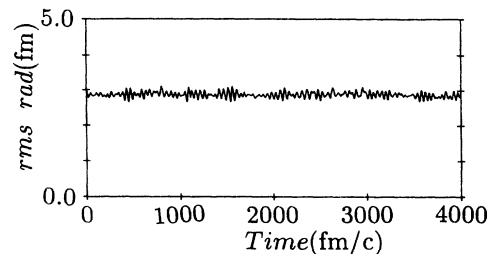


FIG. 1. The time evolution of the rms radius of the ¹⁶O nucleus.

evolution of the rms radius of our ^{16}O nucleus.

Two ^{16}O nuclei which we have successfully constructed are then boosted towards each other as in the following way. Once the center-of-mass incident energy $E_{\text{c.m.}}$ and the impact parameter b are given, the Coulomb trajectory of the relative motion is determined in the phase space of coordinate and momentum. We fix the initial value of the relative distance R to be $R=20$ fm. Then the initial position $\mathbf{D}_1=(X_1, Y_1, Z_1)$ on the Coulomb trajectory of one ^{16}O nucleus is given as follows in the coordinate system on the x - z plane whose origin is the center of mass and whose z axis is along the beam direction:

$$\begin{aligned} X_1 &= \frac{R}{2} \sin\theta, \quad Y_1 = 0, \quad Z_1 = \frac{R}{2} \cos\theta, \\ \theta &\equiv |\cos^{-1}(1/\epsilon)| - |\cos^{-1}[(1+d/R)/\epsilon]|, \\ d &\equiv (l/8e)^2/\mu, \quad l \equiv b(2\mu E_{\text{c.m.}})^{1/2}, \quad \mu = 8m, \\ \epsilon &\equiv [1 + d \cdot 2E_{\text{c.m.}}/(8e)^2]^{1/2}, \end{aligned} \quad (2.8)$$

where m stands for the nucleon mass. The initial velocity $\dot{\mathbf{D}}_1=(\dot{X}_1, \dot{Y}_1, \dot{Z}_1)$ of this ^{16}O nucleus at \mathbf{D}_1 is given as

$$\begin{aligned} \dot{X}_1 &= -V_r \cos\theta - V_\theta \sin\theta, \quad \dot{Y}_1 = 0, \\ \dot{Z}_1 &= -V_r \sin\theta + V_\theta \cos\theta, \\ V_r &\equiv \frac{1}{2} \left[\frac{2}{\mu} \left(E_{\text{c.m.}} - \frac{l^2}{2\mu R^2} - \frac{(8e)^2}{R} \right) \right]^{1/2}, \\ V_\theta &\equiv \frac{1}{2} \frac{l}{\mu R}. \end{aligned} \quad (2.9)$$

The initial position $\mathbf{D}_2=(X_2, Y_2, Z_2)$ and velocity $\dot{\mathbf{D}}_2=(\dot{X}_2, \dot{Y}_2, \dot{Z}_2)$ of the other ^{16}O nucleus are given by

$$\mathbf{D}_2 = -\mathbf{D}_1, \quad \dot{\mathbf{D}}_2 = -\dot{\mathbf{D}}_1. \quad (2.10)$$

III. THE COLLISIONLESS QMD AND FUSION WINDOW

It is well known^{16,17,14} that the time-dependent Hartree-Fock (TDHF) calculation of the heavy-ion collision yields the result that, in the incident energy region higher than some threshold energy E_{th} , the fusion process does not take place in some low partial wave region, $0 \leq l \leq l_<$. The values of E_{th} and $l_<$ depend on the colliding nuclei and the effective two-nucleon force and $l_<$ increases with the increase of the incident energy. Thus the fusion takes place in the region of the partial wave, $l, l_< \leq l \leq l_>$, which is called the fusion window. However it has been discussed that the incorporation of the effects of two-nucleon collisions into the mean field pushes up the value of E_{th} to much higher energy than the TDHF calculation¹⁸ or will even deny the existence of the low- l cutoff $l_<$.¹⁹ Experimentally, up to now all searches for the existence of the low- l cutoff $l_<$ in fusion have been negative.²⁰⁻²⁵

In this section we report the results of the study about the $^{16}\text{O}+^{16}\text{O}$ fusion reaction with the QMD without two-nucleon collisions. The incident energy region we treat is from the sub-Coulomb-barrier energy up to

$E_{\text{lab}}=220$ MeV. The main aim of our study is to check whether or not the collisionless QMD gives rise to the fusion window. Namely, we aim to compare the collisionless QMD calculations with the TDHF ones. As we will show in the next section, the QMD calculation including the two-nucleon collisions denies the existence of the fusion window. Thus the calculation with the collisionless QMD is useful for the study of the role of two-nucleon collisions in the fusion reaction.

We remember that a fusion event in the TDHF calculations is defined rather operationally as the event in which the coalesced one-body density survives through one or more rotations of the composite system or through several oscillations of its radius.¹⁶ Since the aim of this section is the comparison of the collisionless QMD calculations with the TDHF ones, we here in this section follow the definition of the fusion in the TDHF method. To adopt this definition of the fusion also in the present QMD approach means that the incomplete fusion process in which one or a few nucleons or clusters escape prior to the formation of the fused system is also regarded to belong to the category of the fusion process.

We denote by T_f the time span during which the fused one-body density rotates once or oscillates its radius several times. The length of T_f depends on the incident energy and the impact parameter. The final states of the collision at the end of the time span of the length T_f have been found to be classified into two categories in the present region of the incident energy: One is the above-defined fusion process which consists of the complete fusion and the incomplete fusion processes. The other category consists of the quasielastic, deep-inelastic-collision-like, and passing-through (or flow-through) processes. By the word, passing-through process, we mean the non-peripheral collision process which ends in two separating nuclei whose mass numbers are not far from 16. The classification into these two categories can be made with almost no ambiguity, because it is very rare that the mass number of the remnant nucleus²⁶ of the incomplete fusion process is near or less than 25 and also it is very rare that the mass numbers of two separating nuclei in the passing-through process are out of the mass number region, $13 \leq A \leq 19$.

We have calculated at least 30 events for each set of the incident energy and the impact parameter. The fusion probability P_f is the ratio of the number of the fusion events to the number of the total events. When the number of the fusion events is close to that of the nonfusion events, we have increased the number of the total events from 30 to 40 or 50.

In Fig. 2 we show the calculated results with the collisionless QMD. The closed circles denote the angular momenta for which the fusion probability is calculated to be 0.5. The curves are drawn so as to connect these closed circles smoothly and we can well regard that these curves indicate the angular momenta for which $P_f=0.5$. At the incident energies at which the closed circles are displayed, we have certified that P_f is larger than 0.5 for the angular momenta between upper and lower curves while P_f is smaller than 0.5 both for the angular momenta larger than the upper curve and for those smaller than

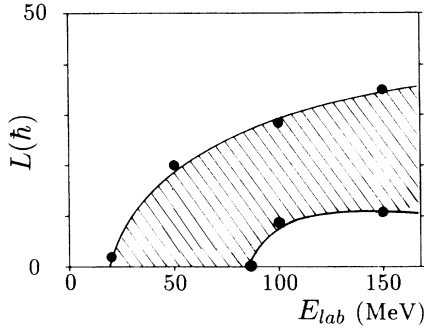


FIG. 2. Angular momentum limits to fusion in the $^{16}\text{O} + ^{16}\text{O}$ reaction calculated with the collisionless QMD. The upper and lower curves indicate the angular momenta for which the fusion probability P_f is 0.5. The partial waves for which P_f is larger than 0.5 are confined in the hatched region between two curves.

the lower curve. Therefore we can well regard that the partial waves that do fuse are confined in the angular momentum region (hatched region) between two curves. Thus we have found that the collisionless QMD gives rise to the fusion window.

The reaction mechanism which gives rise to the transparency in the partial wave region below the lower curve is the passing-through process. This situation is entirely the same as in the TDHF calculations.

When we compare our results with those of the TDHF calculations of Ref. 27, we see that the behavior of the upper and lower curves in Fig. 2 is qualitatively similar to that of the $l_>$ and $l_<$ values of the TDHF calculation. However, if quantitatively compared, we note that the threshold energy E_{th} of Fig. 2 which is 87 MeV in the laboratory frame is larger than $E_{\text{th}} = 54$ MeV of the TDHF calculation. We consider that this difference of the E_{th} values may be partly due to the difference of the effective nuclear force used here from that used in the TDHF calculation. This is because it is reported that the amount of dissipation and hence the E_{th} value in the TDHF calculation depend sensitively on the effective nuclear force.²⁸

IV. FUSION AND ITS FADE OUT

We report in this section the results of the investigation of the fusion process with the QMD with inclusion of two-nucleon collisions. The region of the incident energy we have treated is the same as in Sec. III, namely, from the sub-Coulomb-barrier energy up to $E_{\text{lab}} = 220$ MeV.

The fusion cross section σ_f has been calculated by the following formula

$$\sigma_f = \frac{\pi}{k^2} \int dl (2l+1) P_f(l) = 2\pi \int db \cdot b P_f(b), \quad (4.1)$$

where $P_f(b)$ [$P_f(l)$] stands for the fusion probability for the impact parameter b (the angular momentum l). $P_f(b)$ has been estimated by $\hat{P}_f(b)$

$$P_f(b) \approx \hat{P}_f(b),$$

$$\hat{P}_f(b) \equiv \frac{n}{N}, \quad (4.2)$$

where n is the number of the complete fusion events and N the number of the total events. The reliability of the estimation of Eq. (4.2) can be studied by calculating the width parameter ΔP_f of the confidence interval

$$|P_f(b) - \hat{P}_f(b)| \leq \Delta P_f. \quad (4.3)$$

When we require that Eq. (4.3) holds true with the confidence coefficient 90%, the value of ΔP_f is given by

$$\Delta P_f = 1.64 \times \left[\frac{n(N-n)}{N^3} \right]^{1/2}. \quad (4.4)$$

The discrimination of the complete fusion event and also the classification of the remaining reaction events have been done as we describe below. We first determine the time span T_f for each set of E_{lab} and b just in the same way as in Sec. III: Namely, by selecting a typical complete fusion event we observe the time interval from the first contact of two nuclei until the fused one-body density rotates once or oscillates its radius several times. We adopt this time interval as T_f . In the present energy region of $E_{\text{lab}} \lesssim 220$ MeV, the final states of the collision at the time T_f after the first contact of two nuclei have been found to be due to the following four reaction process; complete fusion, incomplete fusion, deep-inelastic-collision-like and quasielastic processes. This result means that the QMD with two-nucleon collisions included does not give rise to the passing-through process which the collisionless QMD predicts as we discussed in Sec. III. Thus the QMD with inclusion of two-nucleon collisions denies the existence of the low- l cutoff $l_<$ in fusion.

In the category of the complete fusion process we have included such process where one or a few nucleons escape within the time span T_f after the fused total system has been formed. This is because if we exclude such nucleon-escape event from the category of the complete fusion, the calculated fusion probability becomes too much smaller than unity even for the nonperipheral impact parameter in the low incident energy region for which experimentally the fusion probability is known to be almost unity. We consider that there are two reasons for the inclusion of the nucleon escape in the complete fusion event. The first one is the insufficient ability of the present QMD framework to confine nucleons inside the fused system. The other is the nucleon escape which is due to the physical evaporation process. To see this point, we here estimate the life time τ_n of the compound nucleus due to the evaporation of a neutron by the following statistical model formula^{29,30}

$$\tau_n = \frac{\hbar}{\Gamma_n}, \quad \Gamma_n = \frac{T^2}{\pi \epsilon_0} e^{-B_n/T},$$

$$\epsilon_0 \equiv \frac{\hbar^2}{2mR^2}, \quad B_n = 8 \text{ MeV}, \quad R = 1.2 A^{1/3} \text{ fm}, \quad (4.5)$$

$$T = \sqrt{E_x/a}, \quad a = \frac{A}{8} \text{ and } \frac{A}{13},$$

for which we use $E_x = E_{\text{lab}}/2 + Q$, $Q = E_{\text{binding}}(^{32}\text{S}) - 2E_{\text{binding}}(^{16}\text{O}) = 16.5$ MeV and $A = 32$. For the level density parameter a , we have adopted two values $A/8$ and $A/13$ according to the recent experimental study.³¹

The calculated results of τ_n are given in Table I. When we compare τ_n with T_f , we find that for $E_{\text{lab}} = 80 \sim 100$ MeV τ_n is similar to T_f and for higher (lower) E_{lab} τ_n is shorter (longer) than T_f .

Based on the above discussion, the discrimination of the complete fusion event has been made in the following two ways. In the first one (prescription I), an event is regarded to be a complete fusion event if the mass number A_f of the fused system is larger than or equal to 29 at the time $t = 350$ fm/c after the first contact of two ^{16}O nuclei. The reason why we have adopted 29 for the lower limit of A_f at $t = 350$ fm/c is simply due to the demand that the experimental fusion cross section $(\sigma_f)_{\text{exp}}$ at $E_{\text{lab}} = 60$ MeV should be reproduced by the theory. As we will see below, to reproduce $(\sigma_f)_{\text{exp}}$ at $E_{\text{lab}} = 60$ MeV is equivalent to reproducing $(\sigma_f)_{\text{exp}}$ for $E_{\text{lab}} \lesssim 60$ MeV. The second way (prescription II) to determine the complete fusion event is to choose the lower limit of A_f at $t = 350$ fm/c to be 29 for $E_{\text{lab}} \leq 60$ MeV, 28 for $60 < E_{\text{lab}} \leq 140$ MeV and 27 for $140 < E_{\text{lab}} \leq 220$ MeV. The explanation of the second way is as follows: If we believe τ_n in Table I, we have no nucleon evaporation at $T = 350$ fm/c for $E_{\text{lab}} \leq 60$ MeV while for $E_{\text{lab}} = 80, 100, 140$ MeV we may have one nucleon evaporation at $t = 350$ fm/c and for $E_{\text{lab}} = 180, 220$ MeV we may have two nucleon evaporation at $t = 350$ fm/c. It is to be noted that the ansatz of no evaporation of nucleons during 350 fm/c for $E_{\text{lab}} \lesssim 60$ MeV means to regard that the emission of the $(32 - A_f)$ nucleons during 350 fm/c for $E_{\text{lab}} \lesssim 60$ MeV is entirely due to the insufficient ability of the present QMD framework to confine nucleons inside the fused system.

We show in Fig. 3 the fusion probability $P_f(b)$ calculated with the prescription I. In this figure, the closed circles represent $\hat{P}_f(b)$ of Eq. (4.2) and the error bars are the length $2\Delta P_f$ with ΔP_f being given by Eq. (4.4). We see that as the incident energy E_{lab} gets higher than about 80 MeV, $P_f(b)$ become smaller roughly uniformly in the whole region of the impact parameter and $P_f(b)$ in the peripheral region fade away gradually. This energy dependence of $P_f(b)$ calculated with prescription I is similar to that of $P_f(b)$ calculated with prescription II.

In Fig. 4 we compare the observed fusion cross section with the theoretical fusion cross sections calculated in two ways, prescriptions I and II. We see that the agreement between theory and experiments is good.

Now we study about the reaction mechanisms which take the place of the fusion mechanism in the region of $E_{\text{lab}} \gtrsim 80$ MeV. Our QMD calculation shows that the decrease of $P_f(b)$ in the whole region of b for $E_{\text{lab}} \gtrsim 80$ MeV is due to the increase of the incomplete fusion cross sections. To see this point, we show in Fig. 5 the instantaneous number of the emitted nucleons. We see that, as E_{lab} increases, the nucleons emitted in the early stage of the collision increase in number.

In addition to the decrease of $P_f(b)$ in the whole b re-

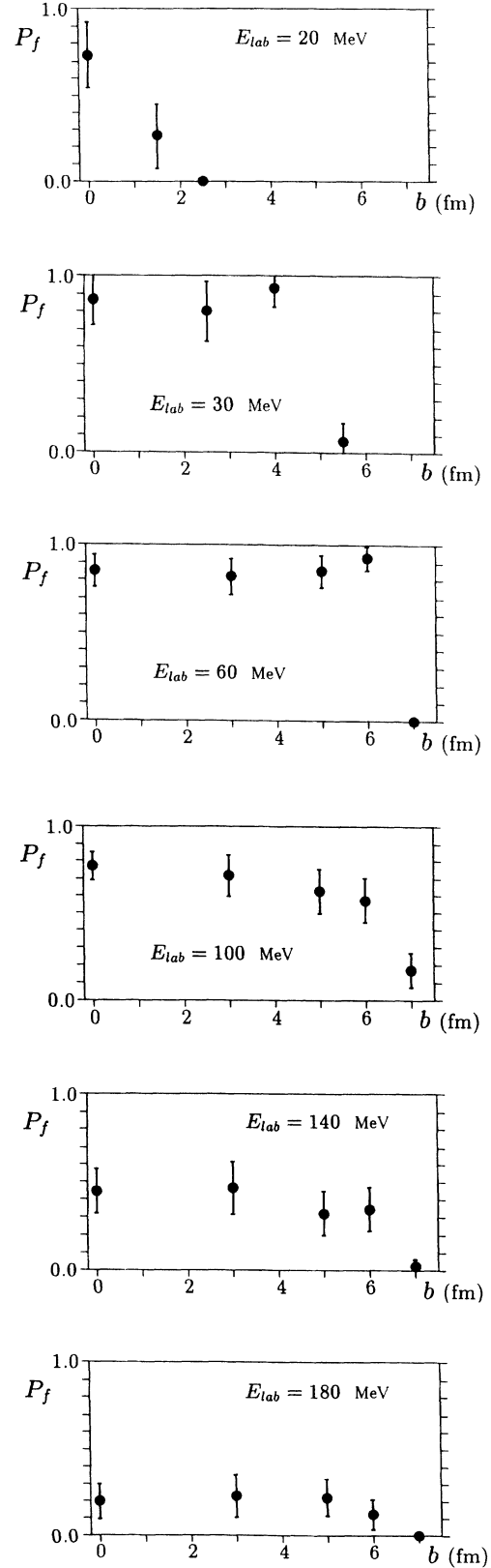


FIG. 3. Fusion probabilities $P_f(b)$ calculated by the use of prescription I in discriminating the fusion events. The closed circles represent $\hat{P}_f(b)$ of Eq. (4.2) and the lengths of the error bars are $2\Delta P_f$ with ΔP_f being given by Eq. (4.4).

TABLE I. The temperature T of the ^{32}S compound nucleus formed by the $^{16}\text{O}+^{16}\text{O}$ collision with the laboratory incident energy E_{lab} and the width Γ_n and life time τ_n due to the neutron decay of the compound nucleus. Two cases of the level density parameter a , $a = A/8$ and $A/13$ ($A=32$), are shown. Units of E_{lab} , T , and Γ_n are MeV while τ_n is in fm/c.

E_{lab}	T	$a = A/8$		T	$a = A/13$	
		Γ_n	τ_n		Γ_n	τ_n
20	2.6	6.6×10^{-2}	3.0×10^3	3.3	2.1×10^{-1}	9.4×10^2
30	2.8	1.0×10^{-1}	1.9×10^3	3.6	3.1×10^{-1}	6.5×10^2
60	3.4	2.5×10^{-1}	8.0×10^2	4.3	6.7×10^{-1}	3.0×10^2
80	3.8	3.7×10^{-1}	5.3×10^2	4.8	9.6×10^{-1}	2.0×10^2
100	4.1	5.2×10^{-1}	3.8×10^2	5.2	1.3	1.5×10^2
140	4.7	8.6×10^{-1}	2.3×10^2	5.9	2.0	9.7×10^1
180	5.2	1.3	1.6×10^2	6.6	2.9	6.9×10^1
200	5.6	1.7	1.2×10^2	7.2	3.7	5.3×10^1

gion, we observe that $P_f(b)$ fade away gradually in the peripheral region as E_{lab} increases. This is not only due to the increase of the incomplete fusion cross section but also due to the increase of the deep-inelastic-collision-like (DIC-like) events. In the region $E_{\text{lab}} \leq 220$ MeV, these DIC-like events do not appear for $b \lesssim 5$ fm, while at $b = 6$ fm they are observed for $E_{\text{lab}} \gtrsim 180$ MeV. Therefore we see that the fade out of the fusion cross section with the increase of the incident energy is due to the increase of the cross section mainly of the incomplete fusion process in the whole region of the impact parameter and partly of the deep-inelastic-collision-like process in the peripheral region.

The decrease of the observed fusion cross section above certain critical energy E_{cr} in lighter heavy-ion systems has been discussed by many authors.³²⁻³⁸ In these discussions, the decrease of the fusion cross section is attributed to the existence of the critical angular momentum l_{cr} which is deduced in most cases either from the critical distance in the entrance channel³³⁻³⁵ or from the yrast

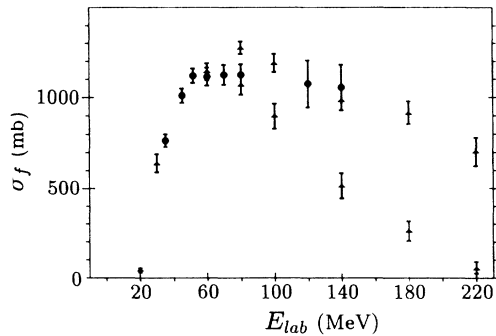


FIG. 4. Comparison of the theoretical fusion cross sections with the experimental ones. The closed triangles with error bars represent the theoretical results and the closed circles with error bars the experimental ones. For $E_{\text{lab}} \geq 80$ MeV, two triangles are shown at the same E_{lab} . The lower one is the result with prescription I while the upper one with prescription II. The error bars attached to the triangles are due to the error bars with the length $2\Delta P_f$ attached to $\hat{P}_f(b)$. The experimental data are taken from Ref. 20 except the ones for $E_{\text{lab}} = 119$ and 141 MeV which are due to Ref. 21.

line^{36,37} (or statistical yrast line³⁸) of the fused system. What is common in these discussions is the assumption that the fusion probability $P_f(l)$ is unity in the region of $0 \leq l \leq l_{\text{cr}}$. On the other hand, our present QMD calculation shows that $P_f(l)$ becomes smaller than unity not only in the peripheral region but also in the central region, as E_{lab} increases in the energy region above certain critical energy \hat{E}_{cr} , although, of course, the statistical factor $(2l+1)$ of $(2l+1)P_f(l)$ makes the contribution of

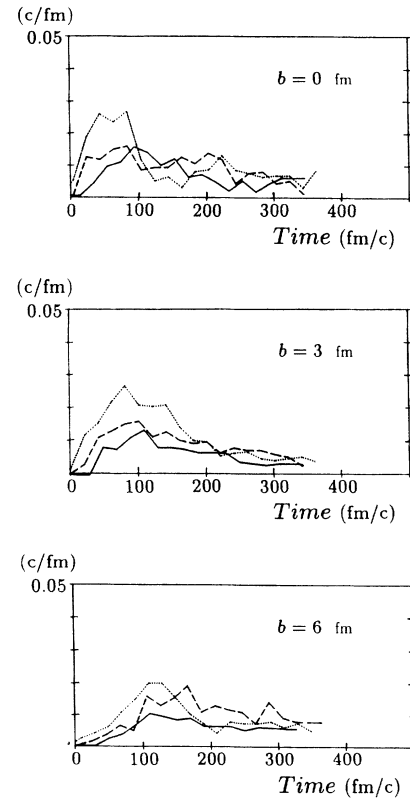


FIG. 5. Instantaneous number of the emitted nucleons. The time interval in which the number is counted is 1 fm/c, hence the unit of the ordinate is c/fm. The solid, dashed, and dotted lines represent the cases of $E_{\text{lab}} = 80, 140,$ and 220 MeV, respectively.

$P_f(l)$ with higher l more important. As for the experimental studies of the role of the entrance-channel angular momentum in incomplete fusion reactions in the region of $E_{\text{lab}} \lesssim 10$ MeV/nucleon, in addition to the indications that incomplete fusion mainly occurs in the peripheral region,^{39,40} there exist also other indications that it may not be limited to peripheral reactions.^{41,42}

V. SUMMARY AND DISCUSSION

By using the QMD (quantum molecular dynamics), we studied the fusion and its fade out in the light heavy-ion system, $^{16}\text{O}+^{16}\text{O}$. In order to treat this kind of low-energy heavy-ion reaction process, the projectile and target nuclei should be constructed to be sufficiently stable. The ^{16}O nucleus we have constructed keeps its stability more than 3000 fm/c. The effective nuclear force we used is the simplified Skyrme-type one. According to the recent study of Ref. 43, this simplified Skyrme-type force gives weak internucleus attraction compared with experiments especially in the low-energy region $E_{\text{lab}} < 20$ MeV/nucleon. One of the main origins of this weak internucleus attraction was attributed in Ref. 43 to the too small radii, hence to the too high densities of the nuclei constructed with this Skyrme-type force compared to experiments. When we use the harmonic oscillator shell model wave function, the root-mean-square (rms) radius of ^{16}O calculated with the present simplified Skyrme-type force is 2.38 fm while the experimental rms radius of ^{16}O is 2.65 fm. In the present QMD approach, however, the size of the nuclear radius is strongly affected by the magnitude of the width parameter L of the nucleon wave packet of Eq. (2.1), and as is shown in Sec. II, the rms radius of our ^{16}O is 2.9 fm which is even larger than the experimental value. Hence we consider that the use of the simplified Skyrme-type force in the present QMD framework does not necessarily mean that the attraction between two ^{16}O nuclei in the present low-energy region is weak compared with experiments.

We first studied about the role of two-nucleon collisions in fusion reaction. We have found that when two-nucleon collisions are switched off, there appears the so-called fusion window as in the TDHF calculations but that with the inclusion of two-nucleon collisions we see nowhere the existence of the low- l cutoff in fusion.

The two-nucleon collision conserves energy and momentum but violates angular momentum conservation due to the isotropic scattering condition. Then one may doubt that the disappearance of the passing-through process may be due to this nonconservation of angular momentum. This is because even in the central collision the incident translational energy may be converted to the energy of the collective rotational motion, and this conversion may lead the system to the fusion. We consider however that it is very unlikely that the sum of the incoherent angular momenta generated by the two-nucleon collision processes is converted into the coherent angular momentum of the collective rotation of the system. In order to resolve this problem, we calculated the angular momentum of $E_{\text{lab}} = 150$ MeV central collision and found that the violation of its conservation along the time span

of 500 fm/c is within about $6\hbar$. In the case without two-nucleon collisions, the low- l cutoff is larger than $10\hbar$ in this energy region. Hence we consider this nonconserved amount about $6\hbar$ is not effective to the disappearance of the passing-through process even if it is totally converted into the collective rotational angular momentum through some unlikely process.

The QMD method simulates the heavy-ion reactions on an event-by-event basis. Thus we calculated the probability $P_f(b)$ of the fusion process for each set of the incident energy E_{lab} and the impact parameter b . This point is a marked contrast to theories such as TDHF and VUU (Vlasov Uehling Uhlenbeck)^{15,44} methods which can give to $P_f(b)$ only two values, 0 or 1. The fusion cross section σ_f due to the calculated $P_f(b)$ was found to be in good accordance with experiments.

The decrease of σ_f with the increase of E_{lab} over 80~100 MeV was found to be due to the decrease of $P_f(b)$ from unity in the whole region of the impact parameter b . The reason of this decrease of $P_f(b)$ was attributed to the increase of the cross section mainly of the incomplete fusion process in the whole range of b and partly of the deep-inelastic-collision-like process in the peripheral region.

How does the reaction mechanism of the $^{16}\text{O}+^{16}\text{O}$ collision evolve when E_{lab} further increases above 220 MeV, which is equal to 13.75 MeV/nucleon? We here report briefly some preliminary results about the QMD study of the above question. Detailed reports will be given elsewhere. We have investigated the collision process up to $E_{\text{lab}} = 225$ MeV/nucleon = 3600 MeV and have traced the time evolution of the collision process up to 400 fm/c after the first contact of two ^{16}O nuclei.

For $b=0$ fm, the incomplete fusion with a compound nucleus formation continues to be a dominant process, but the mass of the compound nucleus decreases continuously with the increase of E_{lab} up to $\sim 40\sim 50$ MeV/nucleon. At $t=400$ fm/c for $E_{\text{lab}}=37.5$ MeV/nucleon, the peak of the distribution of the compound nucleus mass A_f is at $A_f \approx 18$. At $E_{\text{lab}}=75$ MeV/nucleon we observe the events where the incompletely fused system reseparates into two fragments from which nucleons and/or clusters continue to escape. In Ref. 45 which treats the central collision of the $^{40}\text{Ca}+^{27}\text{Al}$ system by the Landau-Vlasov (equivalent to VUU) method, a reaction process similar to the above-mentioned process is reported to occur in the energy region between 35 MeV/nucleon and 50 MeV/nucleon. In this reference it is also reported that below 30 MeV/nucleon, the reaction process is the incomplete fusion process similar to ours. At $E_{\text{lab}}=150$ MeV/nucleon we observe the events where the reseparation of the incompletely fused system is now not into two but into three fragments. This observation is different from the result of Ref. 45 which says that above 50 MeV/nucleon, the incompletely fused system still breaks into two fragments now with large relative velocity. At $E_{\text{lab}}=225$ MeV/nucleon we observe the explosion events.

For $b=3$ fm, the evolution of the reaction mechanism looks similar to that of the central collision up to about 30 MeV/nucleon, but already at $E_{\text{lab}} \approx 30$ MeV/nucleon

we observe the onset of the reseparation process of the incompletely fused system into two fragments. At $E_{\text{lab}} = 75$ MeV/nucleon, in addition to the reseparation process of the fused system into two fragments, we observe the appearance of a new process which is similar to the so-called participant-spectator (PS) reaction process⁴⁶ in high-energy heavy-ion collisions. At $E_{\text{lab}} = 150$ and 225 MeV/nucleon, the reaction process is dominated by the PS-like process.

In the case of $b = 6$ fm, as we have mentioned in Sec. IV, we observe in addition to the incomplete fusion process, the appearance of a deep-inelastic-collision (DIC)-like process at $E_{\text{lab}} \approx 180$ MeV = 11.25 MeV/nucleon. As E_{lab} gets higher, the probability of the DIC-like process increases and DIC-like process tends toward the quasielastic process. For E_{lab} above 75 MeV/nucleon we observe the dominance of the quasielastic process.

As has been discussed by many authors, the fade out of

the fusion reaction is the start of the big evolution of the reaction mechanism occurring in the energy region, 10 MeV/nucleon $\lesssim E_{\text{lab}} \lesssim 100$ (or 200) MeV/nucleon. The QMD simulation shows us quantitatively detailed features of this evolution of the reaction mechanism which are markedly different for different impact parameters. In addition to the present symmetric light heavy-ion system, it is desirable to extend the QMD study similar to the present one also for asymmetric as well as heavy heavy-ion systems.

ACKNOWLEDGMENTS

This work was done partly by the use of the computer facility of the Research Center for Nuclear Physics of Osaka University and also partly by the financial aid by the Institute for Nuclear Study of University of Tokyo.

-
- ¹J. Aichelin and H. Stöcker, Phys. Lett. B **176**, 14 (1986).
²J. Aichelin, G. Peilert, A. Bohnet, A. Rosenhauer, H. Stöcker, and W. Greiner, Phys. Rev. C **37**, 2451 (1988).
³G. Peilert, H. Stöcker, W. Greiner, A. Rosenhauer, A. Bohnet, and J. Aichelin, Phys. Rev. C **39**, 1402 (1989).
⁴J. Aichelin, C. Hartnack, A. Bohnet, L. Zhuxia, G. Peilert, H. Stöcker, and W. Greiner, Phys. Lett. B **224**, 34 (1989).
⁵G. E. Beauvais, D. H. Boal, and J. C. K. Wong, Phys. Rev. C **35**, 545 (1987).
⁶D. H. Boal and J. N. Glosli, Phys. Rev. C **37**, 91 (1988).
⁷D. H. Boal and J. N. Glosli, Phys. Rev. C **38**, 1870 (1980); **38**, 2621 (1988).
⁸D. H. Boal, J. N. Glosli, and C. Wicentowich, Phys. Rev. C **40**, 601 (1989).
⁹L. Wilets, E. M. Henley, M. Kraft, and A. D. Mackellar, Nucl. Phys. A **282**, 341 (1977).
¹⁰R. J. Lenk and V. R. Pandharipande, Phys. Rev. C **34**, 177 (1986).
¹¹C. Dorso, S. Duarte, and J. Randrup, Phys. Lett. B **188**, 287 (1987).
¹²A. Ohnishi, T. Maruyama, and H. Horiuchi (submitted to Phys. Rev. C).
¹³L. Zamick, Phys. Lett. **45B**, 313 (1973).
¹⁴J. W. Negele, Rev. Mod. Phys. **54**, 913 (1982).
¹⁵G. F. Bertsch and S. Das Gupta, Phys. Rep. **160**, 189 (1988).
¹⁶K. T. R. Davies, K. R. S. Devi, S. E. Koonin, and M. R. Strayer, in *Treatise on Heavy-Ion Science*, edited by D. A. Bromley (Plenum, New York, 1984), Vol. 3, p. 1.
¹⁷C. Y. Wong, Phys. Rev. C **25**, 1460 (1982).
¹⁸M. Tohyama, Phys. Rev. C **36**, 187 (1987).
¹⁹P. Grange, J. Richert, G. Wolschin, and H. A. Weidenmüller, Nucl. Phys. A **356**, 260 (1981).
²⁰B. Fernandez, C. Gaarde, J. S. Larsen, S. Pontoppidan, and F. Videbaek, Nucl. Phys. A **306**, 259 (1978).
²¹F. Saint-Laurent, M. Conjeaud, S. Harar, J. M. Loiseaux, J. Menet, and J. B. Viano, Nucl. Phys. A **327**, 517 (1979).
²²A. Lazzarini, H. Doubre, K. T. Lesko, V. Metag, A. Seamster, R. Vandenbosch, and W. Merryfield, Phys. Rev. C **24**, 309 (1981).
²³S. Kox, A. J. Cole, and R. Ost, Phys. Rev. Lett. **44**, 1204 (1980).
²⁴A. Szanto de Toledo, T. M. Cormier, M. Herman, B. Lin, P. M. Stwertka, M. M. Coimbra, and N. Carlin Filho, Phys. Rev. Lett. **47**, 1881 (1981).
²⁵H. Ikezoe, N. Shikazono, Y. Tomita, K. Ideno, Y. Sugiyama, E. Takekoshi, T. Tachikawa, and T. Nomura, Nucl. Phys. A **456**, 298 (1986).
²⁶We defined nuclei (or clusters) according to the linked cluster method as in Ref. 2 or 3.
²⁷P. Bonche, B. Grammaticos, and S. E. Koonin, Phys. Rev. C **17**, 1700 (1978).
²⁸P. G. Reinhard, A. S. Umar, K. T. R. Davies, M. R. Strayer, and S. J. Lee, Phys. Rev. C **37**, 1026 (1988).
²⁹T. E. O. Ericson, Adv. Phys. **9**, 425 (1960).
³⁰P. Bonche, S. Levit, and D. Vautherin, Nucl. Phys. A **427**, 278 (1984).
³¹G. Nebbia, K. Hagel, D. Fabris, Z. Majka, J. B. Natowitz, R. P. Schmitt, B. Sterling, G. Mouchaty, G. Berkowitz, K. Strozewski, G. Viesti, P. L. Gonthier, B. Wilkins, M. N. Namboodiri, and H. Ho, Phys. Lett. B **176**, 20 (1986).
³²U. Mosel, in *Treatise on Heavy-Ion Science* (Ref. 16), Vol. 2, p. 1.
³³J. Galin, D. Guerreau, M. Lefort, and X. Tarrago, Phys. Rev. C **9**, 1018 (1974).
³⁴R. Bass, Nucl. Phys. A **231**, 45 (1974).
³⁵D. Glas and U. Mosel, Phys. Rev. C **10**, 2620 (1974).
³⁶M. Lefort, J. Phys. (Paris) Colloq. **33**, C5-73 (1972).
³⁷S. Harar, in *Nuclear Molecular Phenomena*, edited by N. Cindro (North-Holland, Amsterdam, 1978), p. 329.
³⁸S. M. Lee, T. Matsuse, and A. Arima, Phys. Rev. Lett. **45**, 165 (1980).
³⁹J. Wilczynski, K. Siwek-Wilczynska, J. Van Driel, S. Gonggrijp, D. C. J. M. Hageman, R. V. F. Janssens, J. Lukasiak, R. H. Siemssen, and S. Y. Van Der Werf, Nucl. Phys. A **373**, 109 (1983).
⁴⁰T. Inamura, M. Ishihara, T. Fukuda, and T. Shimoda, Phys. Lett. **68B**, 51 (1977).
⁴¹H. Utsunomiya, T. Nomura, M. Ishihara, T. Sugitate, K. Ieki, and S. Kohmoto, Phys. Lett. **105B**, 135 (1981).
⁴²H. Ikezoe, N. Shikazono, Y. Tomita, K. Ideno, Y. Sugiyama,

- and E. Takekoshi, Nucl. Phys. **A444**, 349 (1985).
- ⁴³T. Wada, S. Yamaguchi, and H. Horiuchi, Phys. Rev. C **41**, 160 (1990).
- ⁴⁴P. Schuck, R. W. Hasse, J. Jaenicke, C. Grégoire, B. Remaud, F. Sébille, and E. Suraud, Prog. Part. Nucl. Phys. **22**, 181 (1989).
- ⁴⁵B. Remaud, C. Grégoire, F. Sébille, and L. Vinet, Phys. Lett. **B 180**, 198 (1986).
- ⁴⁶For example, S. Nagamiya and M. Gyulassy, in *Advances in Nuclear Physics*, edited by J. W. Negele and E. Vogt (Plenum, New York, 1984), Vol. 13, p. 201.